Periodic eclipses of the young star PDS 110 discovered with WASP and KELT photometry

H. P. Osborn,[1][*] J. E. Rodriguez,[2] M. A. Kenworthy,[3] G. M. Kennedy,[4]
E. E. Mamajek,[5,6] C. E. Robinson,[7] C. C. Espaillat,[7] D. J. Armstrong,[1,8]
B. J. Shappee,[9][†] A. Bieryla,[2] D. W. Latham,[2] D. R. Anderson,[10] T. G. Beatty,[11,12]
P. Berlind,[2] M. L. Calkins,[2] G. A. Esquerdo,[2] B. S. Gaudi,[13] C. Hellier,[10]
T. W.-S. Holoien,[11,14][‡] D. James,[15] C. S. Kochanek,[11,14] R. B. Kuhn,[16] M. B. Lund,[17]
J. Pepper,[18] D. L. Pollacco,[1] J. L. Prieto,[19,20] R. J. Siverd,[22] K. G. Stassun,[17,23]
D. J. Stevens,[13] K. Z. Stanek[13,14] and R. G. West[1]

Affiliations are listed at the end of the paper

ABSTRACT

We report the discovery of eclipses by circumstellar disc material associated with the young star PDS 110 in the Ori OB1a association using the SuperWASP and Kilodegree Extremely Little Telescope surveys. PDS 110 (HD 290380, IRAS 05209-0107) is a rare Fe/Ge-type star, an $\sim$10 Myr-old accreting intermediate-mass star showing strong infrared excess ($L_{IR}/L_{bol} \simeq 0.25$). Two extremely similar eclipses with a depth of 30 per cent and duration $\sim$25 d were observed in 2008 November and 2011 January. We interpret the eclipses as caused by the same structure with an orbital period of 808 $\pm$ 2 d. Shearing over a single orbit rules out diffuse dust clumps as the cause, favouring the hypothesis of a companion at $\sim$2 au. The characteristics of the eclipses are consistent with transits by an unseen low-mass (1.8–70 M_{Jup}) planet or brown dwarf with a circumsecondary disc of diameter $\sim$0.3 au. The next eclipse event is predicted to take place in 2017 September and could be monitored by amateur and professional observatories across the world.

Key words: protoplanetary discs – circumstellar matter – stars: individual: PDS 110 – stars: pre-main-sequence – stars: variables: T Tauri, Herbig Ae/Be.

1 INTRODUCTION

The revolution in high-resolution imaging at both near-infrared (NIR; e.g. SPHERE, Beuzit et al. 2008; GPI, Macintosh et al. 2014) and sub-millimeter wavelengths (ALMA, Wootten & Thompson 2009) is providing new insights into the era of planet formation (ALMA Partnership et al. 2015; Rapson et al. 2015; Thalmann et al. 2015). This includes structure in circumstellar discs such as rings, spirals and gaps (e.g. Pinte et al. 2015; Benisty et al. 2017).

The inner regions of discs ($\sim$AU) are still too small to be directly imaged. The transit of dusty circumstellar material in front of a star, however, allows us to resolve the structure of eclipsing material at a resolution limited only by the stellar diameter ($\sim$0.005–0.02 au).

Eclipses have been previously used to detect inner ring edges in circumsecondary discs (ϵ Aur Carroll et al. 1991; EE Cep, Gałan et al. 2012), gas accretion streams from the circumstellar disc (e.g. Bouvier et al. 1999; Cody et al. 2014; Ansdell et al. 2016), sharp outer disc edges in circumsecondary discs (e.g. KH 15D; Herbst et al. 2002) and even ring gaps in putative circumplanetary discs (e.g J1407; Mamajek et al. 2012; Kenworthy & Mamajek 2015).

Unfortunately, these events are rare, with only a dozen or so such eclipsing objects currently known. However, projects like the Wide Angle Survey for Planets (WASP; Pollacco et al. 2006) and the Kilodegree Extremely Little Telescope (KELT; Pepper et al. 2007, 2012) provide long baseline, high-precision time series photometry for a large portion of the entire sky. The combination of baseline, cadence, precision and sky coverage make these surveys well suited to search for these 'Disc Eclipsing' systems. The Disc Eclipse Search with KELT survey has been conducting an archival search for these unique systems in the $\sim$4 million KELT light curves (Rodriguez, Pepper & Stassun 2016c) and has already led to the discovery and

Table 1. Stellar Parameters for PDS 110.

Parameter	Description	Value	Source	Reference(s)
α_{J2000}	Right Ascension (RA)	05:23:31.008	Tycho-2	Høg et al. (2000)
δ_{J2000}	Declination (Dec.)	-01:04:23.68	Tycho-2	Høg et al. (2000)
SpT	Spectral Type	keF6 IVeb	–	Miroshnichenko et al. (1999)
U	Johnson U	11.02	PDS	Gregorio-Hetem & Hetem (2002)
B	Johnson B	10.934 ± 0.005	–	Miroshnichenko et al. (1999), Pojmanski (2002)
B_T	Tycho B_T magnitude	11.093 ± 0.058	Tycho-2	Høg et al. (2000)
V	Johnson V	10.422 ± 0.002	ASAS	Pojmanski (2002)
V_T	Tycho V_T magnitude	10.476 ± 0.048	Tycho-2	Høg et al. (2000)
g'	Sloan g'	10.693 ± 0.032	APASS	Henden et al. (2015)
R	Cousins R	10.10	PDS	Gregorio-Hetem & Hetem (2002)
r'	Sloan r'	10.285 ± 0.01	APASS	Henden et al. (2015)
I	Cousins I	9.77	PDS	Gregorio-Hetem & Hetem (2002)
i'	Sloan i'	10.174 ± 0.017	APASS	Henden et al. (2015)
J	2MASS magnitude	9.147 ± 0.021	2MASS	Skrutskie et al. (2006)
H	2MASS magnitude	8.466 ± 0.042	2MASS	Skrutskie et al. (2006)
K_s	2MASS magnitude	7.856 ± 0.021	2MASS	Skrutskie et al. (2006)
WISE1	WISE 3.4 μm band mag	6.941 ± 0.035	*WISE*	Wright et al. (2010)
WISE2	WISE 4.6 μm band mag	6.474 ± 0.019	*WISE*	Wright et al. (2010)
WISE3	WISE 12 μm band mag	4.512 ± 0.016	*WISE*	Wright et al. (2010)
WISE4	WISE 22 μm band mag	1.809 ± 0.021	*WISE*	Wright et al. (2010)
IRAS 12 μm	IRAS Flux Density (Jy)	0.558 ± 0.056	*IRAS*	Helou & Walker (1988)
IRAS 25 μm	IRAS Flux Density (Jy)	1.68 ± 0.10	*IRAS*	Helou & Walker (1988)
IRAS 60 μm	IRAS Flux Density (Jy)	2.13 ± 0.15	*IRAS*	Helou & Walker (1988)
IRAS 100 μm	IRAS Flux Density (Jy)	1.68	*IRAS*	Helou & Walker (1988)
μ_α	Proper motion in RA (mas yr^{-1})	1.146 ± 1.067	*Gaia*	Gaia Collaboration et al. (2016)
μ_δ	Proper motion in Dec. (mas yr^{-1})	-0.338 ± 1.076	*Gaia*	Gaia Collaboration et al. (2016)
Distance	pc	335 ± 13	*Hipparcos*	Hernández et al. (2005)

analysis of six previously unknown large dimming events including the periodic dimming events around V409 Tau (Rodriguez et al. 2015), DM Ori (Rodriguez et al. 2016d), and an ∼69 yr period analogue to ϵ Aur, TYC 2505-672-1 (Rodriguez et al. 2016b). The OGLE survey of the galactic bulge (Udalski 2003) has also discovered young eclipsing candidates that require follow up (e.g. Scott et al. 2014).

In this paper, we present the light curve of PDS 110, a young star in the Ori OB1 association, which shows two extended, deep dimming events over durations of ∼25 d, separated by about 808 d. We interpret these eclipses as due to the transit of a circumsecondary matter associated with an unseen companion PDS 110b, in a bound Keplerian orbit about PDS 110. In Section 2, we summarize the properties of PDS 110. In Section 3, we present photometric and spectroscopic data obtained for PDS 110. In Section 4, we interpret the spectral and photometric data with main-sequence (MS) fitting, a simple Spectral Energy Distribution (SED) model and a Gaussian eclipse model of the eclipses. In Section 5, we discuss the likely mechanism behind the eclipses, and in Section 6 we cover the prospects for future observations.

2 BACKGROUND ON THE STAR PDS 110

PDS 110 (also known as HD 290380, IRAS 05209-0107, GLMP 91, 2MASS J05233100-0104237 and TYC 4753-1534-1) has been observed in many photometric (Garcia-Lario et al. 1990; Alfonso-Garzon et al. 2012; Hernández et al. 2005) and spectroscopic (MacConnell 1982; Torres et al. 1995; Miroshnichenko et al. 1999; Gregorio-Hetem & Hetem 2002; Rojas, Gregorio-Hetem & Hetem 2008) studies.

It was also found to have a signficant IR excess (Garcia-Lario et al. 1990), representing roughly 25 per cent of the total luminosity

(Rojas et al. 2008), which likely has comparable contributions from a disc and a more spherical envelope (Gregorio-Hetem & Hetem 2002). Table 1 summarizes the photometry we will use here. Spectroscopically, it shows Hα in emission with an equivalent width of roughly 6 Å and LiI 670.7 nm in absorption with an equivalent width of 0.08 m Å (Gregorio-Hetem & Hetem 2002). A range of spectral types have been assigned to it (F0, Cannon & Pickering 1949; keF6IVeb, Miroshnichenko et al. 1999; F7e, Miroshnichenko et al. 1999). Rojas et al. (2008) made estimates of the luminosity, mass and age, but used a distance of 600 pc which is significantly larger than its measured distance (Gaia Collaboration et al. 2016), leading to overestimates of the mass and luminosity and underestimates of the age. The foreground extinction is small, with $E(B - V) = 0.05$ mag (Miroshnichenko et al. 1999).

PDS 110 has a *Gaia* parallax of 2.91 ± 0.34 mas, corresponding to a distance of 345 ± 40 pc, and a negligible proper motion (1.15 ± 1.07, -0.34 ± 1.08) mas yr^{-1} (Gaia Collaboration et al. 2016). This distance makes PDS 110 consistent with being a member of the Ori OB1a association that has an estimated distance of 335 ± 13 pc and similarly small mean proper motion of (0.75 ± 0.29, -0.18 ± 0.22) Wu et al. (2009). The Ori OB1 association has an estimated age of 7–10 Myr (Briceño et al. 2007; Van Eyken et al. 2012; Ciardi et al. 2014; Ingleby et al. 2014). The group contains numerous B stars, but not earlier than B1 (Brown, de Geus & de Zeeuw 1994), suggesting that the age may be slightly higher (10–15 Myr).

3 DATA

In this section, we briefly introduce the photometric and spectroscopic data obtained for PDS-110. Fig. 1 shows full and phase-folded light curves along with views of eclipses observed in 2008 (observed by WASP-North, WASP-South and ASAS) and 2011
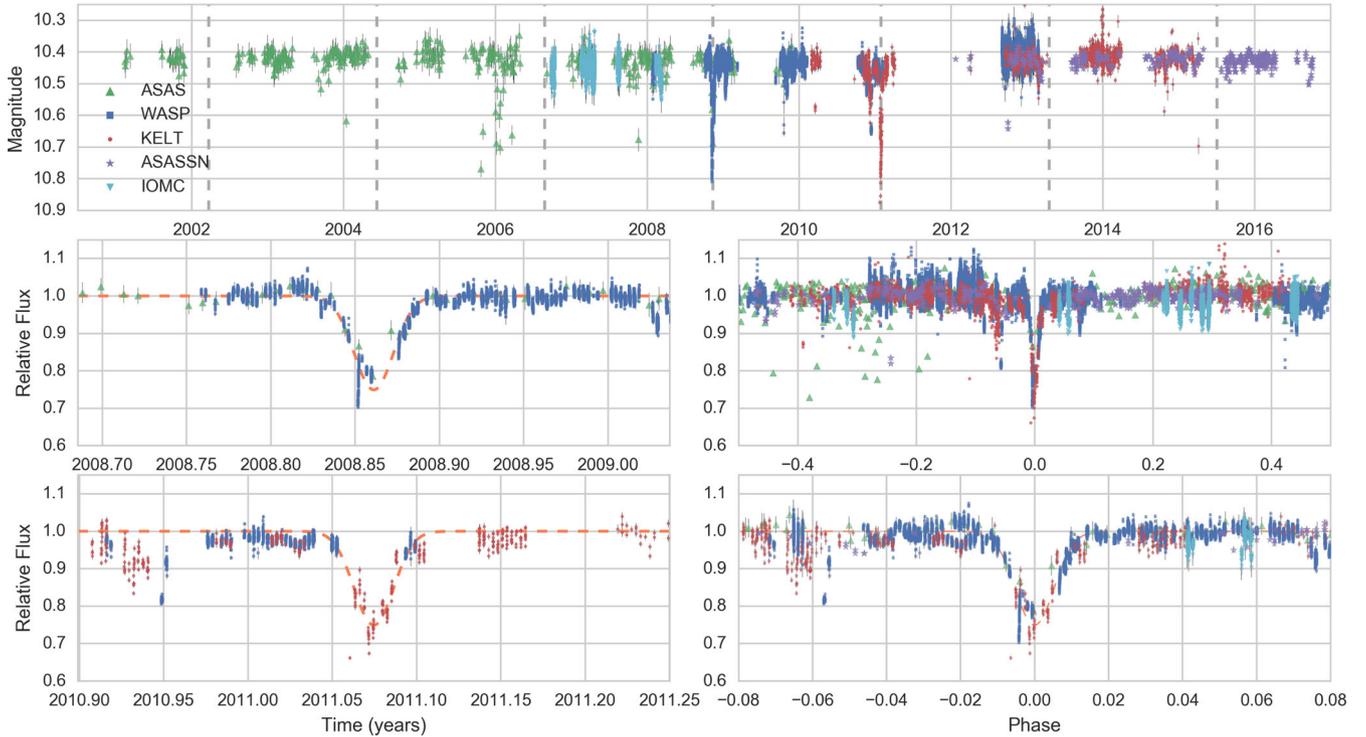
Figure 1. WASP (blue squares), KELT (red circles), ASAS (green triangles), ASAS-SN (purple stars) and IORC (turquoise triangles) observations. Upper figure: plotted from 2002 to 2016. Eclipse times are shown with dashed vertical lines. Lower left figures: individual eclipses in 2008 (upper) and 2011 (lower). Lower right figures: phase-folded light curve with full phase coverage (upper) and zoomed to the eclipse (lower). The best-fitting eclipse model (see Section 4.3) is overplotted in orange in these cases. In all cases, we have applied a vertical offset to the KELT and WASP data to match the quiescent magnitude seen in the ASAS *V* band data. However, there has been no attempt to place all the data on the same absolute scale.
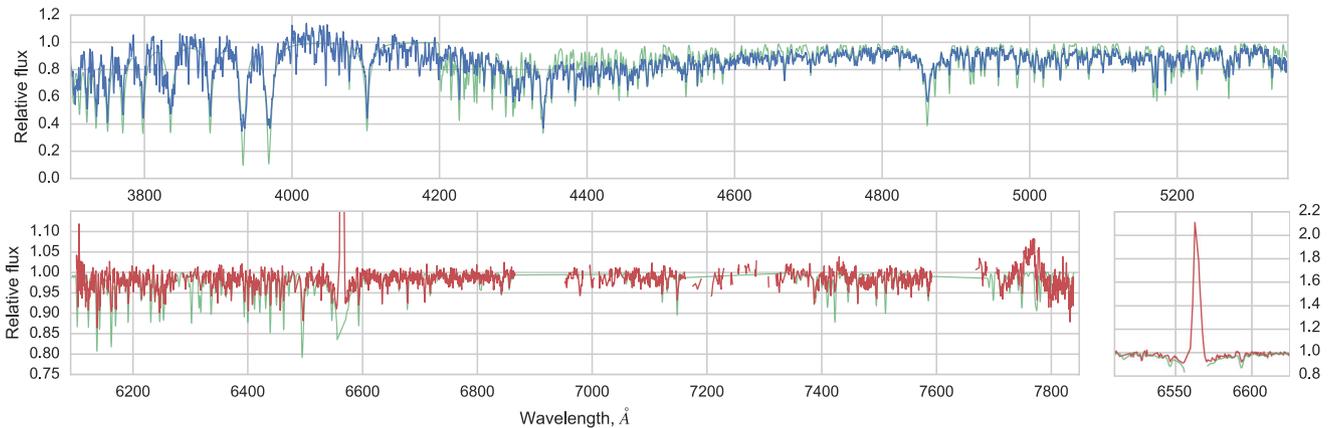

Figure 2. Red and Blue spectra of PDS 110 taken with the WHT/ISIS. The best-fitting synthetic spectrum is shown in green. H α emission is shown in a separate plot in the lower right.

(observed by KELT). If the 2.2-yr separation of the eclipses is a period, all other predicted eclipses lie in an observing gap. Figs 2 and 3 show optical and IR spectroscopy and best-fitting models.

3.1 WASP

The WASP is composed of two outposts, located at the Roque de los Muchachos Observatory on La Palma (WASP-North) and the South African Astronomical Observatory (WASP-South). Each observatory consists of eight cameras using 200 mm f/1.8 lenses and cameras with 2048 × 2048 pixel CCDs, 7.8 × 7.8 deg² fields of view and pixel scales of 13.7 arcsec (Pollacco et al. 2006). Light

curves were detrended using a version of the SysRem algorithm developed specifically for WASP (Tamuz, Mazeh & Zucker 2005; Collier Cameron et al. 2006).

PDS 110 was observed by both WASP-North and WASP-South with exposure times of 30 s and a cadence of 8–10 min. In total, 49558 observations were taken between UT 2008 January 25 and 2013 February 23.

Light curves were further cleaned, initially by removing 3σ anomalies and regions with high hourly scatter (e.g. with hourly rms scatter above 3 per cent). To remove trends present in all nearby stars but not removed by SysRem detrending, nightly linear trends were fitted to the median-divided fluxes of 100 bright and non-varying
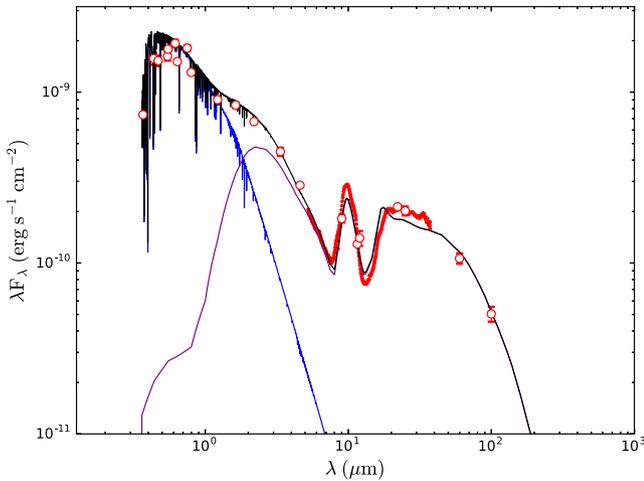
Figure 3. Best-fitting model (black) to the SED of PDS 110. Photometry (red) are from Table 1 and *Spitzer* IRS (Werner et al. 2004; Houck et al. 2004) low-resolution spectra are from the Cornell Atlas of *Spitzer* IRS Sources (CASSIS, Lebouteiller et al. 2011). The best-fitting model includes emission from a NextGen stellar photosphere (Hauschildt, Allard & Baron 1999) (blue) and disc emission (purple).

stars within a 25 arcmin aperture. The target light curve was then divided by these residual trends, improving the average flux rms from 6 per cent to 3 per cent.

3.2 Kelt

The KELT is an all sky, photometric survey of bright stars ($8 < V < 11$) designed to detect transiting planets around bright stars (Pepper et al. 2007, 2012). The project is comprised of two telescopes, KELT-North in Sonoita, AZ, USA and KELT-South in Sutherland, South Africa. Both telescopes have a 42-mm aperture, a broad *R* band filter and observed with a 10–20 min cadence. Using a Mamiya 645-series wide-angle lens with an 80 mm focal length (f/1.9), the telescopes have a 26×26 deg^2 field of view, and a 23 arcsec pixel scale.

PDS 110 is located in KELT-South field 05 ($\alpha = 06^h\,07^m\,48\overset{s}{.}0$, $\delta = +3° \,00'\,00''$). The KELT-South telescope observed PDS 110 from UT 2010 February 28 to UT 2015 April 09, obtaining 2892 observations. For a detailed description of the KELT data acquisition and reduction process, see Siverd et al. (2012) and Kuhn et al. (2016). The typical per-point error is ∼0.02 per cent.

3.3 All-Sky Automated Survey (ASAS)

With the goal of finding and cataloging bright variable stars, the All-Sky Automated Survey (ASAS) obtained photometric observations of a large fraction of the sky. The survey observed simultaneously in two bandpasses (*V* and *I*) from two observing sites, Las Campanas, Chile and Haleakala, Maui. A detailed description of the survey set-up, data acquisition and reduction pipeline is presented in Pojmanski (1997). At each location are two wide-field Minolta 200/2.8 APO-G telephoto lenses and a $2K \times 2K$ Apogee CCD. The telescope and camera set-up corresponds to an 8.8×8.8 deg^2 field of view and a pixel scale of 13.75 arcsec. PDS 110 was observed from 2001 until 2010.[1] There are 488 ASAS epochs with a typical per-point flux error of 3 per cent.

Both KELT and WASP have non-conventional passbands and potential zero-point magnitude offsets. Therefore, to compare them with photometry from other surveys, the out-of-eclipse photometric median was normalized to the out-of-eclipse median of ASAS (Johnson *V* band).

3.4 All-Sky Automated Survey for SuperNovae (ASAS-SN)

The All-Sky Automated Survey for SuperNovae (ASAS-SN) is monitoring the entire sky every two days down to a *V* band magnitude of 17. The survey has two separate observing sites, each with four 14 cm Nikon telephoto lenses and 2k × 2k thinned CCD. The FOV is 4.5×4.5 deg^2 and the pixel scale is 7.8 arcsec. PDS 110 was observed 559 times from 2012 until 2016 with an average per-point rms of 1 per cent. For a complete description of the observing strategy and reduction process, see Shappee et al. (2014).

3.5 *INTEGRAL*–OMC

The INTErnational Gamma-Ray Astrophysics Laboratory (INTE-GRAL; Winkler et al. 2003) is an ESA satellite in orbit since 2002. As well as performing gamma-ray and X-ray observations, INTER-GRAL possesses an Optical Monitoring Camera (OMC; Mas-Hesse et al. 2003), a *V* band (500–600 nm) imager designed to measure the target's optical brightness and position. It observed PDS-110 on 14 occasions from 2006 to 2008, taking over 2000 individual flux measurements with an average cadence of 2.7 min and a median precision of 1.4 per cent (Alfonso-Garzon et al. 2012).[2]

3.6 ISIS spectrum

A low-resolution spectrum of PDS 110 was taken with the ISIS spectrograph in the R600B and R600R modes on the 4.2-m William Herschel Telescope at the ING, La Palma (shown in Fig. 2). The spectrum exhibits a strong Hα emission line, moderate emission in the Ca H & K line cores, and Li I absorption at $\lambda = 670.8$ and 610.3 nm – all consistent with previous measurements (Torres et al. 1995; Rojas et al. 2008). To characterize the spectra, a grid of 1200 synthetic spectra were generated with the PYTHON package ISPEC (Blanco-Cuaresma et al. 2014) using the MARCS model atmospheres (Gustafsson et al. 2008) and compared with the optical spectrum. The best-fitting models had $T_{\text{eff}} = 6500 \pm 250$, $\log(g) \simeq 3.8$ and [Fe/H] $= -0.5 \pm 0.2$, in agreement with previous estimates of the stellar parameters (e.g. 6653 K; Gregorio-Hetem & Hetem 2002).

3.7 TRES spectra

We have taken seven spectra of PDS 110 with the Tillinghast Reflector Echelle Spectrograph (TRES; Fűrész et al. 2008; Szentgyorgyi & Furész 2007) on the 1.5-m telescope at the Fred Lawrence Whipple Observatory, Arizona. The TRES spectra have resolution $R \sim 44\,000$ and were reduced, extracted and analysed with the Spectral Parameter Classification procedure of Buchhave et al. (2012). We ran this without priors for each spectrum (with an average SNR of 53.5) and took a weighted average of the resulting stellar parameters. These give an effective temperature of $T_{\text{eff}} = 6360 \pm 110$ K, a log *g* of 3.89 ± 0.17 and [Fe/H] $= 0.06 \pm 0.06$. Only metallicity

---

[1] ASAS data from http://www.astrouw.edu.pl/asas/?page=aasc

[2] IOMC data accessed from Vizier at http://vizier.cfa.harvard.edu /viz-bin/VizieR?-source=J/A+A/548/A79

Table 2. Determined Stellar Parameters for PDS 110.

M_V	2.54 ± 0.11	$T_{\rm eff}$	6400 ± 150 K
$E(B-V)$	0.09 mag	$\log g$	3.8 ± 0.3
A_V	0.24 ± 0.07	[Fe/H]	0.06 ± 0.06
$\log(L/L_\odot)$	0.89 ± 0.05	R_s	$2.23 \pm 0.18\,R_\odot$
Age	$\sim$11 Myr	M_s	$\sim$$1.6\,M_\odot^N$
$\upsilon \sin i_*$	64.3 ± 0.9		

shows a significant difference from previous estimates of stellar parameters. The higher precision of the TRES spectrum suggests that this value is more precise, and we adopt it here. The star is rapidly rotating with $\upsilon \sin i_*$ of $64.3 \pm 0.9\,{\rm km\,s^{-1}}$.

4 ANALYSIS

4.1 Hertzsprung–Russell diagram position

Previously published spectral types span F5–F7 (Miroshnichenko et al. 1999; Suárez et al. 2006; Rojas et al. 2008). Based on the $T_{\rm eff}$ scale for pre-MS stars from Pecaut & Mamajek (2013), a spectral type of F6 (± 1 subtype) translates to a $T_{\rm eff}$ estimate of 6250 ± 140 K. Based on these estimates, we adopt a mean $T_{\rm eff}$ of 6450 ± 200 K.

On the scale of Pecaut & Mamajek (2016), this temperature translates to a V band bolometric correction of ${\rm BC}_V \simeq -0.02 \pm 0.02$ mag. Fitting the UBV photometry listed in Table 1 alone, the range of quoted spectral types translates to a reddening of $E(B-V) \simeq 0.09$ mag. Combining this estimate along with the two previous independent reddening estimates from Section 2, we adopt a mean reddening estimate of $E(B-V) \simeq 0.07 \pm 0.02$ and V band extinction of $A_V \simeq 0.24 \pm 0.07$ mag.

Adopting the mean distance to the Ori OB1a from Hernández et al. (2005) as representative for PDS 110, we can now calculate stellar parameters like absolute magnitude ($M_V = 2.54 \pm 0.11$), apparent bolometric magnitude ($m_{\rm bol} = 10.14 \pm 0.08$), absolute bolometric magnitude ($M_{\rm bol} = 2.52 \pm 0.11$), luminosity ($\log(L/L_\odot) = 0.89 \pm 0.05$ dex) and radius ($R = 2.23 \pm 0.18\,R_\odot$). Interpolating between the pre-MS isochrones from Siess, Dufour & Forestini (2000), the stellar mass is $1.6\,M_\odot^N$ and its age of $\sim$11 Myr, consistent with the rest of Ori OB1a.

4.2 SED disc model

To model the SED of PDS 110, we used the self-consistent irradiated, accretion disc models of D'Alessio et al. (2006) to create a model grid using the stellar parameters of PDS 110 in Table 2. We adopted a dust sublimation temperature of 1400 K to set the inner radius of the disc. We included outer disc radii of 50, 150 and 300 au, viscosity parameters (α) of 0.01, 0.001 and 0.0001 and dust settling parameters (ϵ; i.e. the dust-to-gas mass ratio in the upper disc layers relative to the standard dust-to-gas mass ratio) of 1.0, 0.5, 0.1, 0.01, 0.001 and 0.0001. The minimum grain size in the disc atmosphere was held fixed at 0.005 μm while we varied the maximum grain size between 0.25, 1.0 and 2.0 μm to reproduce the 10 μm silicate emission feature. The inclination angle was fixed at 60°.

Based on the χ-squared values, the best-fitting model has $a_{\rm max} = 0.25\,\mu = m$, $\epsilon = 0.5$, $\alpha = 0.01$ and an outer radius of 300 au. Uncertainties are beyond the scope of this analysis. This disc model has a mass of $0.006\,M_\odot^N$ using equation (38) in D'Alessio et al. (1999). While there are no millimeter data available to provide

spatial constraints, a large outer radius of 300 au is consistent with the significant MIR and FIR excess of this object given that the strength of the disc emission is related to the disc mass, which, in turn, depends on radius (D'Alessio et al. 1999). We also note that $\epsilon = 0.5$ corresponds to a relatively flared disc. Here, we measure a disc height at 2 of 0.3 au.

4.3 Photometry

Some out-of-eclipse variability is seen with peak-to-peak amplitudes on the order of $\sim$3 per cent. From the measured $v\sin(i)$ (64 km s^{-1}), we would naively estimate a $P_{\rm rot}$ of $\sim$1.7 d. However, searches with lomb-scargle periodograms (Press & Rybicki 1989) on both the entire data set and shorter segments do not detect any coherent period of variation attributable to rotation, with the signals dominated by day- and month-aliases from the ground-based surveys. This suggests that variations are stochastic or quasi-periodic, as has been seen for T-Tauri stars before (Rucinski et al. 2008; Siwak et al. 2011). The (space-based) IOMC light curves show candidate signals at 1.11 and 0.304 d, with an amplitude of around 3 per cent. However, like the ground-based data, the time coverage is non-continuous. The KELT light curves alone show a possible signal with $P = 67$ d.

Some dimmings, slightly shallower in depth and shorter in duration than the eclipses (only 3 to 4 points, or 9 to 12 d long) are also seen in ASAS data in 2006. These are inconsistent with the proposed period (see Section 4) seen and the lack of simultaneous data also means, we are unable to rule out whether these are caused by systematics or from a genuine drop in stellar flux.

All observations thus far have also been monochromatic, with the ASAS, KELT and WASP data all focused on the V/R bands, and showing little differences in variability between one another in- or out-of-eclipse.

4.4 Simple eclipse model

The light curve clearly shows two significant dips in 2008 and 2011. The implied period of $\sim$2.2 yr means no observations were made during times of expected eclipses prior or after these two events. The integer multiples of this separation (1.1 yr, 0.73 yr, etc.) would produce observable eclipses in the current data, therefore have been ruled out. We fit a simple Gaussian model to the phase-folded combined photometry to estimate the physical parameters of the eclipse. A Markov chain Monte Carlo model was run to determine uncertainties on the best fit with EMCEE (Foreman-Mackey et al. 2013) in PYTHON. The results of the model, and output posteriors, are shown in Fig. 4. We find the period to be 808 ± 3 d with an eclipse centred at HJD = 2454781 ± 2, depth of 26 ± 6 per cent and full width at half-maximum of 7 ± 2 d. The residuals show that the in-transit variability increases substantially compared to out-of-transit, indicative of finer structure in the eclipse light curve (see Fig. 1).

5 INTERPRETATION AND DISCUSSION

5.1 Summary of information

We have detected two near-identical eclipses of the bright ($V = 10.4$ mag), young ($\sim$10 Myr) star PDS-110 in the OB1a association with WASP, KELT and ASAS photometry. The two events are separated by 808 ± 2 d and have nearly identical shapes, durations ($\sim$25 d) and depths ($\sim$26 per cent). Sharp in-eclipse gradients
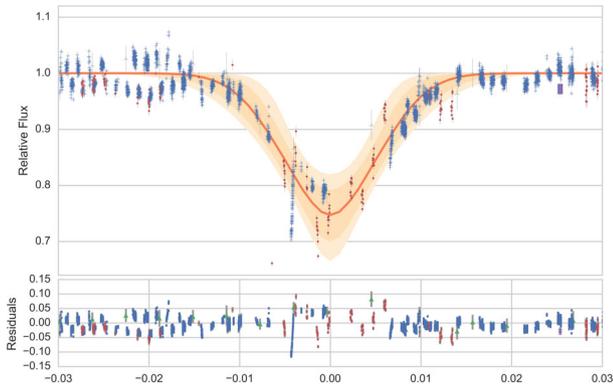
Figure 4. A best-fitting Gaussian model compared to phase-folded data with $1\sigma/2\sigma$ error regions in orange/yellow. Dark blue and red points show measurements from WASP and KELT, respectively, and have been phase-folded on the median period value.

suggest fine structure in the eclipsing material. The similarities of the eclipses strongly suggest that they are periodic. Unfortunately, despite 25 seasons of data across 15 yr and five surveys, all other predicted eclipses lie in observing gaps.

A study of the star and disc suggests that PDS 110 is a young Ge/Fe star surrounded by a thick protoplanetary disc, which contributes to as much as ∼25 per cent of the total luminosity. Since we see significant optical emission and negligible extinction, we must be viewing the star at a significant inclination relative to the stellar disc. Hence, any eclipsing material must reside at a significant altitude above the disc mid-plane.

For any eclipse hypothesis, we must take into account the shallow depth of this eclipse, its interesting substructure and whether the material is optically thick or thin. The most probable explanation is that the occulting object entirely crosses the star, but is optically thin. In this case, the slow and Gaussian-like in- and egress gradients are the result of density gradients within a diffuse occulting dust cloud. Sharp features during the eclipse can be explained as regions of sharply varying density within the cloud, such as gaps, clumps, thicker rings or ring gaps. This would appear the most plausible scenario, although a mix of sharp optically thick regions and low-opacity dust regions, as has been proposed for the J1407b ring system, may also work. These scenarios can be disentangled with multiband photometry during eclipse (see Section 6).

There exist two potential mechanisms for the eclipses. First that circumstellar dust caused the eclipse; and second that the eclipse of a secondary body caused the eclipse. We explore these hypothesis in detail here.

5.2 Circumstellar structure scenario

Many processes within the large circumstellar dust disc could disturb dust above the mid-plane and into eclipse. One possibility is from a spiral arm or a vortex. However, such scenarios are likely concentrated in the disc mid-plane, have significant azimuthal extent (of order radians), and move much more slowly than the material itself, hence not conducive to short, deep eclipses.

KH-15D-like dimmings, in which one member of a binary pair passes behind the circumstellar disc each orbit is another possibility. However, a binary on a 2 yr orbit would clear the entire inner disc region – inconsistent with the disc model needed to explain the SED. If the total obscuration of a companion star leads to an ∼30 per cent dip during eclipse, it must be less than $-2.5^*\log 0.3/0.7$ or only

∼0.9 mag fainter. Hence, such a bright companion would likely have been detected in either the CCF of the optical spectra or in the SED model.

Although the mechanism of eclipse remains unsolved, the deep and aperiodic dimmings or UX Ori stars (known as UXORs), which are seen around many Herbig Ae/Be stars (Bertout 2000) are similar to the eclipses seen in PDS-110. Some eclipses resemble a single PDS-110 eclipse in depth or duration (e.g. Caballero 2010). However, these dimming events tend to be deeper (often several magnitudes), longer duration (weeks to years) and are aperiodic. Light curves of those UXORs found also tend to exhibit many events, usually with differing depths and durations.

The proposed mechanisms for UXOr-like dimming events include hydrodynamical fluctuations at the inner edge of self-shadowed circumstellar discs (Dullemond et al. 2003), occultations of dust clumps in their circumstellar disc (Grinin 1988; Voshchinnikov 1989; Grady et al. 2000, etc.), and the eclipsing debris of planetesimal collisions in young asteroid belts (Kennedy et al. 2017). As an F-type star there is no guarantee that the self-shadowing proposed as a cause of UXOr behaviour is present for PDS-110. Our tentative SED fit also suggests an unsettled ($\epsilon = 0.5$) and moderately turbulent ($\alpha = 0.01$) disc – atypical for UXORs (Dullemond & Dominik 2004). Regardless, the inferred period for the events, and their rarity, suggests the occulting material lies well beyond the disc's inner edge at the sublimation radius. The lack of other significant variability suggests that the occulting material lies well above the 'main' disc, and that the disc structure may be relatively unimportant for determining the nature of the eclipses.

While this style of eclipse does not fit what is observed for PDS-110, it is possible that we could be observing a new UXOr-like eclipse behaviour.

Regardless of the formation mechanism, any diffuse clumps would be subject to shear. The angular shear rate is $\mathrm{R}d\Omega/dR = -3\Omega/2$, so across a clump of radius R_{cl} the shear velocity is $v_{\mathrm{sh}} = 6\pi R_{\mathrm{cl}}/P$ (where P is the orbital period). That is, a clump of any size will be sheared out by a factor of 6π after one orbit, and the radial and vertical optical depth will be roughly 6π times lower. Any disc structure will shear out rapidly, and on successive orbits will have a very different azimuthal extent. Thus, the similar shapes of the eclipses mean that if they were caused by the same clump, an additional means to maintain the concentration of this clump is needed.

5.3 Circumsecondary structure scenario

We have therefore established that the eclipsing object is highly likely to be periodic, and unlikely to be formed of streams or clumps of dust. The simplest way of concentrating material is with the gravitational attraction of a massive body. This is the established interpretation for many long-duration eclipses in young systems, with orbits from 48 d (Herbst et al. 1994) to ∼70 yr (Rodriguez et al. 2016a). We explore here the likely characteristics of such a body by considering its Hill Sphere.

5.3.1 Hill Sphere Considerations

With an orbital period of $P = 808$ d, and a total mass of 1.6 solar masses, we derive a circular Keplerian velocity of $27\,\mathrm{km\,s^{-1}}$. By assuming an eclipse is caused by an optically-thick knife-edge moving across the star, the gradient of the steepest slope can be used to give a minimum velocity of the eclipsing object. For the sharp flux increase seen at 2008.85 (∼20 per cent in 6 h) in WASP data
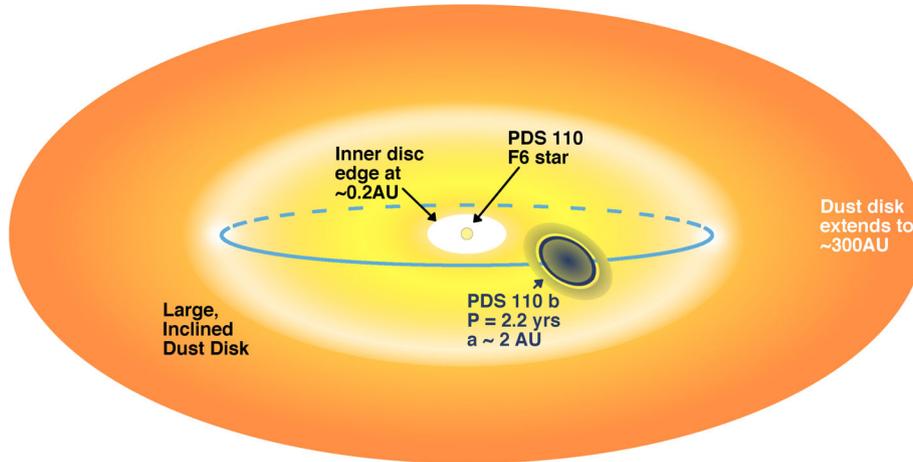
Figure 5. A sketch of the PDS 110 system. The primary star is surrounded by a warm disc of dust inclined away from edge-on. Orbiting around the primary star is a secondary companion with an extended disc which eclipses the primary every 808 d.

(Fig. 1), this gives $v_{min} = 13\,km\,s^{-1}$. This is therefore consistent with the implied orbital motion of $27\,km\,s^{-1}$ as an optically thin or angled structure could produce faster velocities for a given slope. From the Keplerian orbital speed and eclipse duration ($\sim$21 d), we can derive the diameter of the eclipsing object to be $\sim$0.3 au, or about 50 million km. A lower limit on the mass of the secondary companion can be derived assuming that the cloud is within the Hill sphere of the secondary.

The Hill radius can be approximated as $a_H \approx a(1-e)(m/3M_s)^{1/3}$, where a is the orbital semimajor axis, e is the orbital eccentricity, m is the mass of the secondary and M_s is the primary (stellar) mass. If the duration of the eclipse is t_{ecl} days, then the diameter of the disc $d_{disc} = v_{circ}t_{ecl}$ and the circular velocity of the companion $v_{circ} = 2\pi a/P$. Combining these expressions with Kepler's third law, the mass of the secondary companion is: $m = 2M_s\,(\pi t_{ecl}/\xi P)^3$, where P is the orbital period of the secondary companion and $0 \leq \xi \leq 1.0$ is the fraction of the Hill sphere that the disc fills. $\xi = 0.3$ is typical for a prograde rotating disc (Nesvorný et al. 2003).

Assuming $M_s = 1.6\,M_\odot^N$ and $t_{ecl} = 21$d and $P = 808$ d gives: $m = 1.8M_{Jup}(1/\xi)^3$ Using the prograde stability criterion of $\xi = 0.3$ (Quillen & Trilling 1998), the mass is 68 M_{Jup} and for $\xi = 0.6$, this becomes 8.5 M_{Jup}. Increasing the eclipse duration (e.g. by including the shallow dips seen 15–20 d before and after) will substantially increase this mass limit (to $>20\,M_{Jup}$ in the case of a 40 d eclipse).

Such a body would likely also perturb a gap in the circumstellar disc at 2.2 au. We recomputed the SED model with a narrow gap at this radius and found it to be consistent with the data, with negligible difference to a gapless model.

5.3.2 Inclination considerations

The two eclipses have similar duration of $\sim$25 d and so we assume that the cloud has a constant size. We hypothesize that the eclipse is caused by the passage of a large optically thin cloud that contains an unseen secondary companion, which holds the cloud together in dynamic equilibrium, and that the companion and cloud orbit around the primary.

In the cases of KH-15D, ϵ Aur and EE Cep, the secondaries are stars, whereas for J1407 the massive body at the centre of the disc appears to be of planetary or brown dwarf mass. In order to cause the eclipse, either of the following two conditions should be fulfilled:

(1) The secondary body is large and on an orbit with low mutual inclination to the disc, but with highly inclined (Uranus-like) circumsecondary material, which protrudes above the circumprimary disc and passes our line of sight of the primary star. If, as our lack of reddening suggests, we are viewing PDS-110 at an angle moderately inclined from edge-on ($\sim$30°), the eclipsing secondary disc must be greater than $\sim$1 au in radius, hence stellar in mass. This, it would likely be detected as anomalous flux in the optical spectra and SED fit.

(2) The secondary body is small but has significant orbital inclination with respect to the disc. Such an orbital scenario could occur due to scattering. This is our favoured scenario, and would be invisible except during eclipse. A figure representing this scenario PDS 110 system is shown in Fig. 5.

5.3.3 Circumplanetary ring model

The WASP eclipse shows substructure over individual nights in the form of steep gradients similar to those seen towards J1407 (Mamajek et al. 2014). While the interpretation is uncertain, we briefly consider the implications of a circumplanetary ring model using the framework of Kenworthy & Mamajek (2015). The rapid changes seen in eclipse, reminiscent of J1407 (Mamajek et al. 2012), could be interpreted as the passage of a Hill sphere filling ring system around a secondary companion, passing across the line of sight of the star. To explore whether such a mechanism could explain the PDS 110 eclipse, we applied the exoring fitting method of Kenworthy & Mamajek (2015) to the WASP eclipse light curve.

We consider the light curve slopes in the WASP and KELT light curves separately. We set the mid-point of the WASP eclipse as 2454 780.7 d, as determined by the Gaussian fit carried out in Section 4.2, and we take the centre of the KELT eclipse to be at 2455 590.4 d, determined by visual inspection of the two light curves and adjusting them so that the photometry of the different epochs gives the most consistent match in both photometry and in the matching of the light-curve gradients. The measurements of light-curve gradient as a function of time from the centre of the respective WASP and KELT eclipses are shown in Fig. 6. The figure shows that there are seven light-curve gradients above 0.1 Lstar d^{-1} during the ingress of PDS 110b, compared to only one during egress. WASP detects five slopes and KELT detects three significant slopes. From this we conclude that many more steep gradients are seen
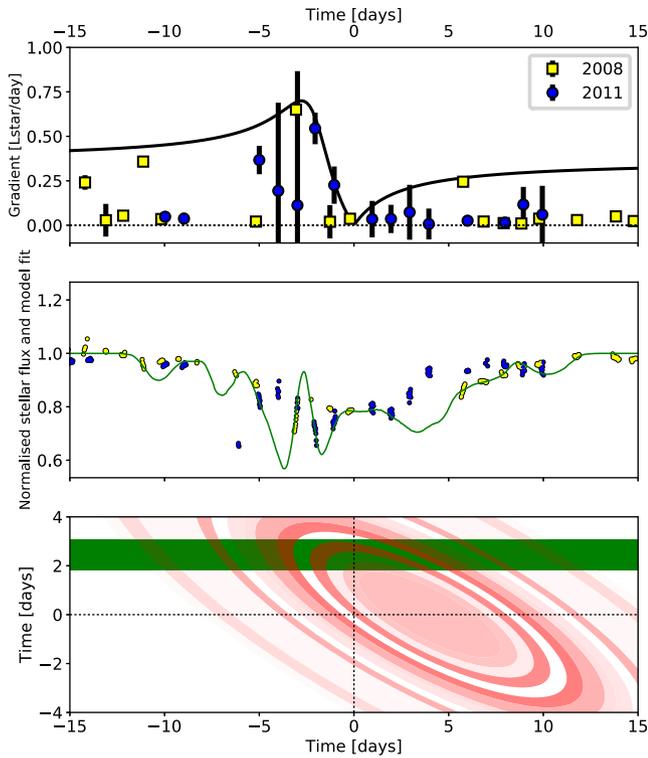
Figure 6. A circumsecondary ring model for PDS 110b. Upper panel: The light-curve gradients seen in 2008 and 2011 photometry (yellow and blue) are shown, along with an upper bound fit to the gradients (black) from which the orientation of the system is derived. Central panel: The photometry in 2008 and 2011 together with the one plausible ring transmission model (green line). Lower panel: A schematic of the model ring system (red nested ellipses) crossing the stellar disc (green).

during ingress in both eclipse events, and in the context of the ring models, this implies an eclipsing object with small spatial scale structure similar to that seen in J1407b. These gradients are used to determine the orientation of the ring system following the method of Kenworthy & Mamajek ([2015](#)) (Section 3.1). By fitting the measured gradients g(t) to the model gradients G(t), we achieve the fit shown in Fig. [6](#) as the solid black curve. All gradients must lie on or below this curve for there to be a consistent ring model. The determined disc parameters have an Impact parameter of 2.45 d, a ring centre offset of 4.02 d (both in velocity space), an apparent disc inclination of 74° and total obliquity of the disc plane to the orbital plane of 26°.

We then model the ring radii and transmissions as the convolution of the stellar disc ($R = 2.23\,R_\odot$) with the ring parameters. Minimization of ring transmissions produced the ring model as seen in Fig. [6](#).

The incomplete coverage of both eclipse events leads to several plausible ring solutions, of which we show just one in Fig. [6](#). The ring model fits both epochs well in several places, and shows deviations in others. From the plot of light-curve gradients, where we can see several high gradients on the ingress of the transit in both epochs, we conclude that a tilted disc containing azimuthal structure at high spatial frequencies is a reasonable fit to the data. There isn't a unique solution using azimuthally symmetric structures, which may be due to several causes: (i) We are seeing at different clocking angles in successive transits (e.g. from a spiral pattern), (ii) the intrinsic stochastic variability of the parent star is affecting the derived photometry and light-curve gradients, (iii) precession of the

disc between successive transits and (iv) the eclipses are instead aperiodic dimmings caused by unexplained dust disc processes. A comprehensive photometric monitoring campaign during future eclipses will help resolve these ambiguities in the interpretation of this object.

6 FUTURE OBSERVATIONS

While we favour the presence of dust structure around a periodic secondary companion as the cause of the eclipses, additional data are needed to test it. In particular, the next eclipse will take place on HJD = 2458015.5 ± 10 (2017 September 9–30). Unfortunately, it will only be observable for a few hours each night from the ground, and space-based observations may be needed for better temporal coverage of the event. The presence or absence of an eclipse will immediately settle the question of periodicity.

High cadence and low noise light curves during the eclipse will better constrain the presence of any smaller scale structures in the eclipsing material, potentially confirming the hypothesis that it is a disc of material with gaps and other structures orbiting a low mass secondary. Colour information during the eclipse can determine if the obscuration is due to small dust grains or larger bodies that produce more achromatic absorption. The continuing out-of-eclipse monitoring by photometric surveys may detect other eclipsing structures and further characterize any other variability.

A secondary should produce radial velocity variations in the primary of ∼200 m s^{-1} (for a $10\,M_{\rm Jup}$ companion) that may be measurable. The difficulty is that the fast rotation and variability of the primary will limit the precision of radial velocity measurements. While the scales corresponding to the orbit of the potential secondary (∼2 au) cannot be resolved in sub-millimeter observations, they can characterize the disc on larger scales (10s of au) and search for distortions or gaps in the outer disc that might indicate the presence of other massive bodies in the system.

7 CONCLUSIONS

We have detected two near-identical eclipses of the bright ($V = 10.4$ mag), young (∼10Myr) star PDS-110 in the OB1a association with WASP, KELT and ASAS photometry. Further ASAS-SN and IOMC photometry of the star have increased the photometric coverage of this star to 25 seasons of data across 15 yr. We interpret these eclipses to be caused by the same optically-thin clump of material on a 808 ± 2 d orbit around the star.

Despite a large circumstellar disc around PDS-110, such a scenario cannot be caused by lose clumps of dust above the disc plane, as shearing forces would not maintain the eclipse depth and duration across 2.2 yr. Therefore, we interpret the eclipse structure to be gravitationally bound around a companion body, which must have mass $> 1.8\,M_{\rm Jup}$.

Such a body must be significantly inclined relative to the circumstellar disc to eclipse the star. The body may be surrounded by rings, as has been hypothesized for J1407, with the sharp photometric gradients seen at $t_0 \pm 5$ d being the result of the transit of a ring gap. This hypothesis can be tested, and the orbiting body studied in much greater detail, in 2017 September when we predict the next eclipse to take place.

and Irregular Transits' workshop in 2016. HPO was funded by a University of Warwick Chancellor's Scholarship. Work performed by JER was supported by the Harvard Future Faculty Leaders Post-doctoral fellowship. GMK is supported by the Royal Society as a Royal Society University Research Fellow. Early work on KELT-North was supported by NASA Grant NNG04GO70G. JAP and KGS acknowledge support from the Vanderbilt Office of the Provost through the Vanderbilt Initiative in Data-intensive Astrophysics. This work has made use of NASA's Astrophysics Data System and the SIMBAD data base operated at CDS, Strasbourg, France. This paper is under review for unlimited release (URS265682). DJA acknowledges funding from the European Union Seventh Framework programme (FP7/2007- 2013) under grant agreement No. 313014 (ETAEARTH). Work by BSG was partially supported by NSF CA-REER Grant AST-1056524. Work by KGS was supported by NSF PAARE grant AST-1358862. EEM acknowledges support from the NASA NExSS program. Part of this research was carried out at the Jet Propulsion Laboratory, California Institute of Technology, under a contract with the National Aeronautics and Space Administration. TW-SH is supported by the DOE Computational Science Graduate Fellowship, grant number DE-FG02-97ER25308. CSK and KZS are supported by NSF grants AST-1515876 and AST-1515927. This research made use of Astropy, a community-developed core Python package for Astronomy (Astropy Collaboration et al. 2013).

REFERENCES

Alfonso-Garzon J., Domingo A., Mas-Hesse J. M., Gimenez A., 2012, A&A, 548, A79

ALMA Partnership et al., 2015, ApJ, 808, L3

Ansdell M. et al., 2016, ApJ, 816, 69

Astropy Collaboration et al., 2013, A&A, 558, A33

Benisty M. et al., 2017, A&A, 597, A42

Bertout C., 2000, A&A, 363, 984

Beuzit J.-L. et al., 2008, in SPIE Astronomical Telescopes+ Instrumentation. p 701418.

Blanco-Cuaresma S., Soubiran C., Heiter U., Jofré P., 2014, A&A, 569, A111

Bouvier J. et al., 1999, A&A, 349, 619

Briceño C., Hartmann L., Hernández J., Calvet N., Vivas A. K., Furesz G., Szentgyorgyi A., 2007, ApJ, 661, 1119

Brown A. G. A., de Geus E. J., de Zeeuw P. T., 1994, A&A, 289, 101

Buchhave L. A. et al., 2012, Nature, 486, 375

Caballero J. A., 2010, A&A, 511, L9

Cannon A. J., Pickering E., 1949, The Henry Draper (HD) Catalogue, Vol.112: HD Extension. Astronomical Observatory of Harvard College, Cambridge, MA

Carroll S. M., Guinan E. F., McCook G. P., Donahue R. A., 1991, ApJ, 367, 278

Ciardi D. R. et al., 2014, in American Astronomical Society Meeting Abstracts# 223.

Cody A. M. et al., 2014, AJ, 147, 82

Collier Cameron A. et al., 2006, MNRAS, 373, 799

D'Alessio P., Cantó J., Hartmann L., Calvet N., Lizano S., 1999, ApJ, 511, 896

D'Alessio P., Calvet N., Hartmann L., Franco-Hernández R., Servín H., 2006, ApJ, 638, 314

Dullemond C., Dominik C., 2004, A&A, 417, 159

Dullemond C. P., van den Ancker M. E., Acke B., van Boekel R., 2003, ApJ, 594, L47

Foreman-Mackey D., Hogg D. W., Lang D., Goodman J., 2013, PASP, 125, 306

Fűrész G., Szentgyorgyi A. H., Meibom S., 2008, Precision of Radial Velocity Surveys using Multiobject Spectrographs — Experiences with Hectochelle. Springer, Berlin Heidelberg, p. 287

Gaia CollaborationBrown A. G. A., Vallenari A., Prusti T., de Bruijne J., Mignard F., Drimmel R., co-authors., 2016, A&A, 595, A2

Gałan C. et al., 2012, A&A, 544, A53

Garcia-Lario P., Manchado A., Suso S. R., Pottasch S. R., Olling R., 1990, A&AS, 82, 497

Grady C. A., Sitko M. L., Russell R. W., Lynch D. K., Hanner M. S., Perez M. R., Bjorkman K. S., de Winter D., 2000, in Mannings V., Boss A.P., Russell S. S., eds, Protostars and Planets IV, Univ. Arizona Press, Tucson, AZ, p. 613

Gregorio-Hetem J., Hetem A., 2002, MNRAS, 336, 197

Grinin V. P., 1988, Sov. Astron. Lett., 14, 27

Gustafsson B., Edvardsson B., Eriksson K., Jørgensen U. G., Nordlund Å., Plez B., 2008, A&A, 486, 951

Hauschildt P. H., Allard F., Baron E., 1999, ApJ, 512, 377

Helou G., Walker D. W. eds, 1988, Infrared Astronomical Satellite (IRAS) Catalogs and Atlases. Volume 7: The small scale structure catalog, p. 1

Henden A. A., Levine S., Terrell D., Welch D. L., 2015, American Astronomical Society Meeting Abstracts. p. 336.16

Herbst W., Herbst D. K., Grossman E. J., Weinstein D., 1994, AJ, 108, 1906

Herbst W. et al., 2002, PASP, 114, 1167

Hernández J., Calvet N., Hartmann L., Briceno C., Sicilia-Aguilar A., Berlind P., 2005, AJ, 129, 856

Houck J. R. et al., 2004, ApJS, 154, 18

Høg E. et al., 2000, A&A, 355, L27

Ingleby L., Calvet N., Hernández J., Hartmann L., Briceno C., Miller J., Espaillat C., McClure M., 2014, ApJ, 790, 47

Kennedy G. M., Kenworthy M. A., Pepper J., Rodriguez J. E., Siverd R. J., Stassun K. G., Wyatt M. C., 2017, R. Soc. Open Science, 4, 160652

Kenworthy M. A., Mamajek E. E., 2015, ApJ, 800, 126

Kuhn R. B. et al., 2016, MNRAS, 459, 4281

Lebouteiller V., Barry D., Spoon H., Bernard-Salas J., Sloan G., Houck J., Weedman D., 2011, ApJS, 196, 8

MacConnell D. J., 1982, A&AS, 48, 355

Macintosh B. et al., 2014, Proc. Natl. Acad. Sci., 111, 12661

Mamajek E. E., Quillen A. C., Pecaut M. J., Moolekamp F., Scott E. L., Kenworthy M. A., Collier Cameron A., Parley N. R., 2012, AJ, 143, 72

Mas-Hesse J. et al., 2003, A&A, 411, L261

Miroshnichenko A., Ivezić Ž., Vinković D., Elitzur M., 1999, ApJ, 520, L115

Nesvorný D., Alvarellos J. L., Dones L., Levison H. F., 2003, AJ, 126, 398

Pecaut M. J., Mamajek E. E., 2013, ApJS, 208, 9

Pecaut M. J., Mamajek E. E., 2016, MNRAS, 461, 794

Pepper J. et al., 2007, PASP, 119, 923

Pepper J., Kuhn R. B., Siverd R., James D., Stassun K., 2012, PASP, 124, 230

Pinte C., Dent W. R., Menard F., Hales A., Hill T., Cortes P., de Gregorio-Monsalvo I., 2015, ApJ, 816, 25

Pojmanski G., 1997, Acta Astron., 47, 467

Pojmanski G., 2002, Acta Astron., 52, 397

Pollacco D. L. et al., 2006, PASP, 118, 1407

Press W. H., Rybicki G. B., 1989, ApJ, 338, 277

Quillen A., Trilling D., 1998, ApJ, 508, 707

Rapson V. A., Kastner J. H., Millar-Blanchaer M. A., Dong R., 2015, ApJ, 815, L26

Rodriguez J. E. et al., 2015, AJ, 150, 32

Rodriguez J. E. et al., 2016a, AJ, 151, 29

Rodriguez J. E. et al., 2016b, AJ, 151, 123

Rodriguez J. E., Pepper J., Stassun K. G., 2016c, in Kastner J. H., Stelzer B., Metchev S. A., eds, IAU Symposium Vol. 314, Young Stars & Planets Near the Sun. Kluwer, Dordrecht, p. 167

Rodriguez J. E. et al., 2016d, ApJ, 831, 74

Rojas G., Gregorio-Hetem J., Hetem A., 2008, MNRAS, 387, 1335

Rucinski S. M. et al., 2008, MNRAS, 391, 1913

Scott E. L., Mamajek E. E., Pecaut M. J., Quillen A. C., Moolekamp F., Bell C. P. M., 2014, ApJ, 797, 6

Shappee B. J. et al., 2014, ApJ, 788, 48

Siess L., Dufour E., Forestini M., 2000, A&A, 358, 593

Siverd R. J. et al., 2012, ApJ, 761, 123

Siwak M. et al., 2011, MNRAS, 410, 2725

Skrutskie M. F. et al., 2006, AJ, 131, 1163

Suárez O., García-Lario P., Manchado A., Manteiga M., Ulla A., Pottasch S. R., 2006, A&A, 458, 173

Szentgyorgyi A., Furész G., 2007, The 3rd Mexico-Korea Conference on Astrophysics: Telescopes of the Future and San Pedro Mártir. Instituto de Astronomia Universidad Nacional Autonoma de Mex, p. 129

Tamuz O., Mazeh T., Zucker S., 2005, MNRAS, 356, 1466

Thalmann C. et al., 2015, ApJ, 808, L41

Torres C. A. O., Quast G., de La Reza R., Gregorio-Hetem J., Lepine J. R. D., 1995, AJ, 109, 2146

Udalski A., 2003, Acta Astron., 53, 291

Van Eyken J. C. et al., 2012, ApJ, 755, 42

Voshchinnikov N. V., 1989, Astrophys., 30, 313

Werner M. et al., 2004, ApJS, 154, 1

Winkler C. et al., 2003, A&A, 411, L1

Wootten A., Thompson A. R., 2009, Proc. IEEE., 97, 1463

Wright E. L. et al., 2010, AJ, 140, 1868

Wu Z.-Y., Zhou X., Ma J., Du C.-H., 2009, MNRAS, 399, 2146

[1] *Department of Physics, University of Warwick, Gibbet Hill Road, Coventry CV4 7AL, UK*

[2] *Harvard–Smithsonian Center for Astrophysics, 60 Garden Street, Cambridge, MA 02138, USA*

[3] *Leiden Observatory, Leiden University, PO Box 9513, NL-2300 RA Leiden, the Netherlands*

[4] *Institute of Astronomy, University of Cambridge, Madingley Road, Cambridge CB3 0HA, UK*

[5] *Jet Propulsion Laboratory, California Institute of Technology, M/S 321-100, 4800 Oak Grove Dr., Pasadena, CA 91109, USA*

[6] *Department of Physics and Astronomy, University of Rochester, Rochester, NY 14627, USA*

[7] *Department of Astronomy, Boston University, One Silber Way, Boston, MA 02215, USA*

[8] *ARC, School of Mathematics and Physics, Queen's University Belfast, University Road, Belfast BT7 1NN, UK*

[9] *Las Cumbres Observatory Global Telescope Network, 6740 Cortona Dr., Suite 102, Santa Barbara, CA 93117, USA*

[10] *Astrophysics Group, Keele University, Staffordshire ST5 5BG, UK*

[11] *Department of Astronomy and Astrophysics, The Pennsylvania State University, 525 Davey Lab, University Park, PA 16802, USA*

[12] *Center for Exoplanets and Habitable Worlds, The Pennsylvania State University, 525 Davey Lab, University Park, PA 16802, USA*

[13] *Department of Astronomy, The Ohio State University, Columbus, OH 43210, USA*

[14] *Center for Cosmology and AstroParticle Physics (CCAPP), The Ohio State University, 191 W.Woodruff Ave., Columbus, OH 43210, USA*

[15] *Astronomy Department, University of Washington, Box 351580, Seattle, WA 98195, USA*

[16] *South African Astronomical Observatory, PO Box 9, Observatory 7935, South Africa*

[17] *Department of Physics and Astronomy, Vanderbilt University, 6301 Stevenson Center, Nashville, TN 37235, USA*

[18] *Department of Physics, Lehigh University, 16 Memorial Drive East, Bethlehem, PA 18015, USA*

[19] *Nucleo de Astronoma de la Facultad de Ingeniera, Universidad Diego Portales, Av. Ejercito 441, Santiago, Chile*

[20] *Millennium Institute of Astrophysics, Santiago, Chile*

[21] *Carnegie Observatories, 813 Santa Barbara Street, Pasadena, CA 91101, USA*

[22] *Las Cumbres Observatory Global Telescope Network, 6740 Cortona Dr., Suite 102, Santa Barbara, CA 93117, USA*

[23] *Department of Physics, Fisk University, 1000 17th Avenue North, Nashville, TN 37208, USA*

This paper has been typeset from a TEX/LATEX file prepared by the author.